THE JOURNAL OF BIOLOGICAL CHEMISTRY
Vol. 277, No. 25, Issue of June 21, pp. 22156–22167, 2002

Printed in U.S.A.

Regulation of Stress Response Signaling by the N-terminal Dishevelled/EGL-10/Pleckstrin Domain of Sst2, a Regulator of G Protein Signaling in *Saccharomyces cerevisiae**

Received for publication, March 7, 2002, and in revised form, March 21, 2002
Published, JBC Papers in Press, April 8, 2002, DOI 10.1074/jbc.M202254200

Scott A. Burchett‡§, Paul Flanary‡¶, Christopher Aston‖, Lixin Jiang‖, Kathleen H. Young‖, Peter Uetz‡‡, Stanley Fields**§§¶¶, and Henrik G. Dohlman‡¶‖‖**

*From the ‡Department of Pharmacology, Yale University School of Medicine, New Haven, Connecticut 06536, ‖Neuroscience Research, Wyeth Ayerst-Research, CN 8000, Princeton, New Jersey 08543-8000, and the **Departments of Genetics and Medicine and §§Howard Hughes Medical Institute, University of Washington, Seattle, Washington 98195*

All members of the regulator of G protein signaling (RGS) family contain a conserved core domain that can accelerate G protein GTPase activity. The RGS in yeast, Sst2, can inhibit a G protein signal leading to mating. In addition, some RGS proteins contain an N-terminal domain of unknown function. Here we use complementary whole genome analysis methods to investigate the function of the N-terminal Sst2 domain. To identify a signaling pathway regulated by N-Sst2, we performed genome-wide transcription profiling of cells expressing this fragment alone and found differences in 53 transcripts. Of these, 40 are induced by N-Sst2, and nearly all contain a stress response element (STRE) in the promoter region. To identify components of a signaling pathway leading from N-Sst2 to STREs, we performed a genome-wide two-hybrid analysis using N-Sst2 as bait and found 17 interacting proteins. To identify the functionally relevant interacting proteins, we analyzed all of the available gene deletion mutants and found three (*vps36*Δ, *pep12*Δ, and *tlg2*Δ) that induce STRE and also repress pheromone-dependent transcription. We selected *VPS36* for further characterization. A *vps36*Δ mutation diminishes signaling by pheromone as well as by downstream components including the G protein, effector kinase (Ste11), and transcription factor (Ste12). Conversely, overexpression of Vps36 enhances the pheromone response in *sst2*Δ cells but not in wild type. These findings indicate that Vps36 and Sst2 have opposite and opposing effects on the pheromone and stress response pathways, with Vps36 acting downstream of the G protein and independently of Sst2 RGS activity.

All cells have the capacity to respond to chemical and sensory stimuli in their environment. In many cases, signal detection occurs through cell surface receptors coupled to G proteins. One particularly well characterized example is the pheromone response pathway in yeast (1). In this case, haploid **a** and α cell types each secrete a peptide pheromone that binds to receptors on cells of the opposite type. Pheromone stimulation leads to activation of a G protein, which entails GTP binding and dissociation of the Gα and $\beta\gamma$ subunits. The G$\beta\gamma$ moiety activates downstream signaling events required for mating, including alterations in gene transcription, morphological and cytoskeletal changes, and cell cycle arrest in G_1. Among the induced genes is *SST2*, which encodes a feedback regulator that stimulates G protein GTPase activity and G protein inactivation (1).

Over the past 5 years, an extensive family of Sst2-related proteins has been identified in higher eukaryotes (2). In every instance examined, the region of core-RGS[1] homology is both necessary and sufficient for G protein GTPase activating function (3). Some RGS proteins contain additional domains or motifs that may be recognized by proteins other than Gα (4–13). The RGS protein p115RhoGEF has one domain that acts as a GTPase-accelerating protein for $G_{13}\alpha$ and a second domain that acts as a GDP-GTP exchange factor for RhoA (14, 15). Other RGS proteins including Egl-10, Eat-16, RGS6, RGS7, RGS9, RGS11, and FlbA, have large N-terminal segments containing a conserved Dishevelled, Egl-10, and pleckstrin (DEP) domain (16). Sst2 has two such DEP regions, composed of residues 50–135 and 279–358. The function of the RGS DEP domains is not known, but in at least two cases (Egl-10, Sst2) they appear necessary and sufficient for membrane localization (17, 18). In the case of Sst2, the N-terminal domain can be expressed as a separate entity, the result of an endoproteolytic processing event *in vivo* (18).

Our objective here was to establish a signaling function for the DEP domain of Sst2, designated N-Sst2. With the completion of the yeast genome sequence, approaches to the identification of new signaling pathways have changed dramatically. Analysis of gene function has become more comprehensive and systematic and can occur at several levels. First, closely related protein isoforms can be identified through sequence similarity analysis or through complementation of gene mutations by functionally similar genes. Second, transcriptional changes can

* This work was supported by a pilot grant from the Claude D. Pepper Center of Yale University (to S. A. B.) and National Institutes of Health Grants P41 RR11823 (to S. F.) and GM55316 and GM59167 (to H. G. D.). The costs of publication of this article were defrayed in part by the payment of page charges. This article must therefore be hereby marked "*advertisement*" in accordance with 18 U.S.C. Section 1734 solely to indicate this fact.

§ Present address: NCI, National Institutes of Health, Neuro-Oncology Branch, Convent Dr., Bldg. 36, Rm. 3B-02, Bethesda, MD 20892.

¶ Present address: Dept. of Biochemistry and Biophysics, University of North Carolina, 405 Mary Ellen Jones Bldg., Campus Box 7260, Chapel Hill, NC 27599-2852.

‡‡ Present address: Institut für Genetik, Forschungszentrum Karlsruhe, PO Box 3640, D-76021 Karlsruhe, Germany.

¶¶ An Investigator of the Howard Hughes Medical Institute.

‖‖ An Established Investigator of the American Heart Association. To whom correspondence should be addressed: Dept. of Biochemistry and Biophysics, University of North Carolina at Chapel Hill, 405 Mary Ellen Jones Bldg., Campus Box 7260, Chapel Hill, NC 27599-2852. Tel.: 919-843-6894; Fax: 919-966-2852; E-mail: henrik_dohlman@med.unc.edu.

[1] The abbreviations used are: RGS, regulator of G protein signaling; DEP, Dishevelled, Egl-10, and pleckstrin; STRE, stress response element; MES, 4-morpholineethanesulfonic acid; PRE, pheromone response element; STRE, stress response element; MAP, mitogen-activated protein; PX, Phox homology; EAP, elongation factor-associated protein; PIPES, 1,4-piperazinediethanesulfonic acid.

be monitored under various physiological conditions, through the use of RNA hybridization arrays (19). Third, signaling complexes can be identified through the use of two-hybrid screens (20, 21) or through the isolation and sequencing of multiprotein complexes (22–26). Fourth, the functional significance of each signaling component can be determined through gene disruption mutations (27).

There are, however, limitations to each of these methods. For instance, transcription analysis can reveal how different physiological conditions affect a particular signaling pathway but cannot be used to identify the components of that pathway. Two-hybrid analysis can reveal the components of a pathway, but it cannot be used to determine how physiological changes affect the interactions of each component. Thus, a combined analysis, encompassing multiple whole genome approaches, can provide highly complementary information about any cellular process. For instance, a combination of two different high throughput methods, protein interaction mapping and large scale phenotypic analysis, was recently used to identify novel DNA repair and DNA damage checkpoint pathway components in *Caenorhabditis elegans* (28).

Here we have used a combination of transcription profiling, protein interaction mapping, and phenotypic analysis of gene disruption mutants to investigate signaling by the N-terminal Sst2 domain. Our findings indicate that N-Sst2 modulates the stress response and does so through proteins not previously recognized to participate in the mating or stress pathways.

EXPERIMENTAL PROCEDURES

Strains and Plasmids—Standard methods for the growth, maintenance, and transformation of yeast and bacteria and for the manipulation of DNA were used throughout (29). The yeast *Saccharomyces cerevisiae* strains used in this study are YPH499 (*MAT**a** ura3–52 lys2–801^{am} ade2–101^{oc} trp1-Δ63 his3-Δ200 leu2-Δ1*), YDM400 (YPH499, *sst2-Δ2*) (30), BY4741 (*MAT**a** leu2Δ met15Δ ura3Δ*) and BY4741-derived mutants lacking YLR113W (*HOG1*, *SSK3*), YER188W, YGR018C, YGR040W (*KSS1*), YER118C (*SHO1*, *SSU81*), YLR417W (*VPS36*, *VPL11*, *GRD12*, *VAC3*), YML038C (*YMD8*), YMR004W (*MVP1*), YJL057C (*IKS1*), YOR036W (*PEP12*, *VPL6*, *VPT13*, *VPS6*), YDL186W, YDR319C, YOL018C (*TLG2*), YDL180W, YHR158C (*KEL1*), YIL159W (*BNR1*), YOR069W (*VPS5*, *GRD2*, *VPT5*, *PEP10*), YMR077C (*VPS20*, *ASI10*, *CHM6*), YOR089C (*VPS21*, *VPT21*, *YPT51*), and YJR102C (*VPS25*) all from Research Genetics (Huntsville, AL). Gene disruptions were not available for the remaining two-hybrid hits YLR457C (*NBP1*) and YGR172C (*YIP1*).

Expression plasmids used in this study have been described previously and are pRS315 (*CEN*, amp^R, *LEU2*) (31), pRS423 (2 μm, amp^R, *HIS3*) (31), pRS316-ADH (*CEN*, amp^R, *URA3*, *ADH1* promoter/terminator) (32), pRS316-ADH-SST2, pRS316-ADH-SST2-P20L, pRS316-ADH-N-SST2 (*SST2* codons 1–392, plus a Myc epitope tag), pRS316-ADH-C-SST2 (*SST2* codons 411–698), pRS315-ADH-C-SST2 (also known as ADHleu-C-SST2) (18), pRS316-GAL-STE4 (33), and YCp50-STE11–4 (34) (from George Sprague, University of Oregon). Overexpression of *VPS36* and *STE12* was achieved by PCR amplification and subcloning into the pYES2.1/V5-His-TOPO (2 μm, *URA3*, *GAL1* promoter, *CYC1* terminator) (Invitrogen, Carlsbad, CA). Primers used were 5′-GTG TGT TTT GAA AGT CAT TCT-3′ and 5′-ACG AGC AGG TAA TCA AAC CA-3′ (for *VPS36*) and 5′-GAA TTG TCT TGT TCA CCA AGG-3′ and 5′-CTG GCC CGC ATT TTT AAT TC-3′ (for *STE12*). pRS423-HSP12-lacZ was constructed by replacing the *FUS1* promoter (*Bam*HI-*Eag*I fragment) of pRS423-FUS1-lacZ with the *HSP12* promoter (608 bp immediately preceding the initiator AUG), which was isolated through PCR amplification of genomic yeast DNA. The primers used were HSP12F (5′-AAT AAT **CGG CCG** ATC CCA CTA ACG GCC CAG CC-3′) containing a synthetic *Eag*I site (indicated in boldface type) and HSP12R (5′-G CGC **GGA TCC** CCA CTT TCT TTA GCC AT TCT TGT TGT ATT TAG TTT TTT TT-3′) containing a synthetic *Bam*HI site, an idealized translation initiation sequence (A*X*A preceding the initiation codon), and the first five codons of *CYC7* (indicated by underlining) fused in frame with codon 10 of the *lacZ* gene.

Two-hybrid N-Sst2 Bait Plasmid Construction—Oligonucleotides were designed to PCR-amplify the N-terminal portion (amino acids 1–392) of Sst2, using pRS316-ADH-Sst2 as the template, the forward primer (5′-CCG **GAA TTC** ATG GTG GAT AAA AAT AGG ACG-3′, containing a synthetic *Eco*RI site, indicated in boldface type), and the reverse primer (5′-GTA C**CC ATG G**TT ACA TAT GAC CCC TTA ATG TGA A-3′, containing a synthetic *Nco*I site, indicated in boldface type). The 0.9-kbp product was cloned in frame downstream of the *GAL4* DNA-binding domain contained in the yeast two-hybrid bait vector pOBD2 (35).

RNA Isolation and Hybridization—Total RNA was isolated from yeast strains using RNeasy columns (Qiagen, Valencia, CA), and stored at −80 °C. Genomic DNA was removed by DNase digestion of 10 μg of total RNA for 30 min at 37 °C in a 100-μl reaction containing DNase I (1.4 units; Invitrogen), RNase inhibitor (0.1 units; Invitrogen), and dithiothreitol (1 mM) in 1× PCR buffer I (PerkinElmer Life Sciences). DNase was removed by passage through an RNeasy column (Qiagen).

Amplified, biotin-labeled cRNA was produced from total RNA as described (36). Briefly, 10 μg of total RNA was incubated for 10 min at 70 °C with a high pressure liquid chromatography-purified oligo(dT) primer containing a T7 RNA polymerase promoter site (5′-GGC CAG TGA ATT GTA ATA CGA CTC ACT ATA GGG AGG CGG T-3′; from GENSET Inc., La Jolla, CA). Following priming, cDNA was prepared using the SuperScript II cDNA synthesis kit (Invitrogen) with the following conditions: 65 min at 50 °C for first strand synthesis with Superscript II reverse transcriptase, followed by 150 min at 16 °C for second strand synthesis with *Escherichia coli* ligase, *E. coli* polymerase, and RNase H. cDNA was purified by phenol/chloroform extraction followed by removal of the organic fraction using Phase Lock Gel I tubes (5 Prime to 3 Prime Inc., Boulder, CO). Biotin-labeled cRNA was transcribed in an *in vitro* transcription reaction mixture containing T7 RNA polymerase (Epicenter, Madison, WI), bio-11-CTP, and bio-11-UTP (Enzo Laboratories, Farmingdale, NY) for 16 h at 37 °C. The cRNA product was purified by RNeasy column and then quantitated by UV absorbance at 260 nm. 15 μg of cRNA was fragmented for 35 min at 95 °C and then added to a 300-μl hybridization mixture containing bovine serum albumin (0.5 mg/ml) and herring sperm DNA (0.1 mg/ml; Promega, Madison, WI) in 1× MES. To estimate the sensitivity of the oligonucleotide arrays, we included 11 *in vitro* synthesized transcripts (spiked transcripts) in each hybridization (37). 200 μl of hybridization mixture was applied to a Ye6100 subA GeneChip (Affymetrix, Santa Clara, CA), and hybridization was allowed to proceed for 20 h at 45 °C on a rotisserie. The sample was then hybridized sequentially to the Ye6100 subB, subC, and subD designs, comprising ~6400 yeast genes and open reading frames. When hybridization was complete, arrays were stained with streptavidin-conjugated phycoerythrin (Molecular Probes, Inc., Eugene, OR) as described (36). Fluorescence intensity was quantitated using the Affymetrix GeneChip laser scanner.

The resulting array images were captured in the GeneChip version 3.3 software package and reduced to relative expression values (average difference values) for each transcript. The spiked transcripts were used to generate a standard curve of concentration *versus* their average difference values. The abundance of each transcript (stated in terms of control transcripts per total transcripts) ranged from 1:300,000 to 1:1,000, calculated by assuming an average RNA size of 1,000 ribonucleotides. This standard curve was then used to determine the absolute expression level of the yeast transcripts and is presented as RNA copies per million total transcripts. Based on the signal response from these control transcripts, the sensitivity of the arrays ranged between 1:100,000 and 1:200,000. Consequently, expression values below 10 RNA copies per million total transcripts are considered below the limit of accuracy. Final data analysis was performed using Excel (Microsoft Corp., Redmond, WA). Pairwise comparisons generated -fold change values. -Fold change values of >4 were considered to be significant.

The arrays include probe sets representing the 5′ and 3′ regions of the β-actin transcript. The 5′ to 3′ signal ratios were >0.7 across all arrays, indicating that the source RNA was of suitable quality.

Two-hybrid Screening—Transformants containing the N-Sst2-Gal4 fusion plasmid were mated to a set of ~6,000 colonies, each expressing a unique full-length open reading frame fused to the Gal4 activation domain, as described previously (20, 35). The resulting diploids were transferred to selective plates deficient in histidine and monitored after 10 days. Proteins identified in two independent screens were analyzed further.

Growth, Transcription, and Phosphorylation Bioassays—For NaCl-dependent growth inhibition, saturated cultures were diluted to A_{600} ~ 0.2 and grown to A_{600} ~ 0.8 and then treated with either water or 10 μM α-factor (final concentration) for 2 h. 10 μl of cells were spotted onto solid medium containing 0.75 M NaCl (where indicated) either without dilution or diluted 1:10, 1:100, 1:1,000, 1:10,000, and 1:100,000 with water or with 10 μM α-factor (where indicated).

For the pheromone-dependent growth inhibition assay (halo assay), overnight cultures were grown in selective media, and 100 μl was diluted with 2 ml of sterile water, followed by the addition of an equal volume of 1% (w/v) dissolved agar (55 °C), and poured onto an agar plate containing the same medium. Sterile filter discs were spotted with synthetic α-factor pheromone and placed onto the nascent lawn to induce growth arrest. The resulting zone of growth-arrested cells was documented after 2 days.

For pheromone-dependent reporter transcription assays (29), strains were grown for 36 h in standard dextrose-selective medium and then diluted in selective medium containing galactose to induce expression of Vps36, Ste4, or Ste12. Mid-log phase cells were then aliquoted (90 μl) to a 96-well plate and mixed with 10 μl of α-factor for 90 min in quadruplicate. For *HSP12* reporter transcription assays, strains were grown in selective medium to mid-log phase and then aliquoted (85 μl) to a 96-well plate and mixed with 15 μl of 5 M NaCl for 10 min in triplicate. Cells to be treated with NaCl were maintained at room temperature instead of 30 °C to reduce basal activity of the stress response promoter. β-Galactosidase activity was measured by adding 20 μl of a freshly prepared solution of 83 μM fluorescein di-β-D-galactopyranoside (Molecular Probes, Inc.; 10 mM stock in Me_2SO), 137.5 mM PIPES, pH 7.2, 2.5% Triton X-100, and incubating for 90 min at 37 °C. The reaction was stopped by the addition of 20 μl of 1 M Na_2CO_3, and the resulting fluorescence activity was measured at 485-nm excitation, 530-nm emission.

For Hog1 phosphorylation assays, saturated cultures were diluted to $A_{600} \sim 0.4$, grown for an additional 3–4 h, and treated with 0.75 M NaCl (final concentration) for 10 min, as indicated. Cells were treated with 10 mM NaN_3, chilled briefly on ice, and harvested by centrifugation at 2,000 $\times$ g for 10 min at 4 °C. The pellets were resuspended (1.5×10^6 cells/μl) in 1$\times$ SDS-polyacrylamide gel electrophoresis (SDS-PAGE) sample buffer (62.5 mM Tris-HCl, pH 6.8, 10% glycerol, 2% SDS, 1% 2-mercaptoethanol, 0.0005% bromphenol blue) and boiled for 10 min. The cells were disrupted by glass bead vortex homogenization for 4 min and centrifuged at 16,000 $\times$ g for 2 min. The supernatant was collected and stored at −20 °C. Lysates were reheated at 37 °C for 20 min before SDS-PAGE and transfer to nitrocellulose. Immunoblots were probed with the 4G10 anti-phosphotyrosine mouse monoclonal antibody (05-321; Upstate Biotechnology, Inc., Lake Placid, NY) at 1:1,000 dilution and a horseradish peroxidase-conjugated goat anti-mouse antibody (Sigma) at 1:3,000 dilution, carried out as described (29).

Bioinformatics—For each gene demonstrated to be differentially expressed in the microarray analysis, a region upstream of the translation start site (to the nearest stop codon, up to 500 bp) was analyzed for sequence motifs representing possible promoter regulatory elements. Most regulatory elements in yeast are found within this region (38). Alignace was used to search for conserved motifs (39). Genespring (Silicon Genetics, Redwood City, CA) was used to identify predefined motifs. Genespring was also used for statistical analysis, comparing the frequency of a motif in a gene list with the upstream regions of all yeast genes. The Transfac data base (Biobase, Braunschweig, Germany) was used to search for previously identified transcription factor binding sites.

A number of Vps36 protein homologues were identified from the nonredundant GenBank™ data base using the advanced BLAST algorithm and the full-length Vps36 protein sequence as the query. PSI-BLAST was used to detect weaker, but nonetheless biologically significant, homologues to Vps36 (40). Multiple alignments of all the Vps36 homologues were performed with ClustalW (41). The alignment was formatted in Phylip and imported into TREEVIEW for visualization of the Vps36 family (42). Classical basic nuclear localization signals were identified using the World Wide Web version of PSORT II (43). The more sensitive hidden Markov model algorithm utilized in the SMART data base was used to detect additional signaling domains and motifs within Vps36 and its homologues (16).

RESULTS

All signaling pathways regulate gene expression. For instance, in yeast, G protein activation leads to the induction of genes with a pheromone response element (PRE) in their promoter region. One of the induced genes encodes Sst2, which is well known to attenuate G protein signaling through its GTPase accelerating function (44). Regulation of the G protein requires the C-terminal RGS domain, C-Sst2 (18, 30). The function of the N-terminal domain is not known. Our aim was to determine whether N-Sst2 regulates a distinct signaling pathway, perhaps independently of the G protein. To this end, we sought to identify genes whose expression changed substantially in cells containing just the N-Sst2 domain. Our approach was to use oligonucleotide probe microarrays to monitor the mRNA levels of all yeast genes, comparing cells that express N-Sst2 with cells that lack the N-Sst2 domain (express C-Sst2 alone).

An *sst2*Δ mutant strain was transformed with plasmids containing either the N-Sst2 segment (residues 1–392 plus a Myc epitope tag) or the C-Sst2 segment (residues 411–698), as described previously (18). Expression was verified by immunoblot analysis with anti-Myc and anti-Sst2 antibodies, as well as by *in vivo* complementation of the *sst2*Δ mutation, which requires co-expression of both N-Sst2 and C-Sst2. To provide uniform expression under various growth conditions, a constitutive promoter from *ADH1* was used in place of the native (PRE-containing) promoter from *SST2*. Cultures in mid-log phase were collected, and total RNA was isolated. Biotin-labeled cRNA was prepared and hybridized to an Affymetrix GeneChip set representing ~6,400 genes and open reading frames over four separate chips. The arrays were then treated with streptavidin-conjugated phycoerythrin, and fluorescence intensity was measured using the Affymetrix GeneChip laser scanner, as described under "Experimental Procedures."

Expression profiles in cells containing N-Sst2 or C-Sst2 are shown are Table I. A comparison of N-Sst2 versus C-Sst2 revealed a >4-fold difference in 53 independent transcripts (0.82% of all genes), of which 40 increased and 13 decreased ("induced" and "repressed" by N-Sst2, respectively). Fewer differences were observed in cells treated with pheromone or when comparing N-Sst2 or C-Sst2 with full-length Sst2 (Fig. 1).[2] Thus, N-Sst2 is necessary for the transcriptional regulation of a discrete set of genes.

We then examined whether the 53 genes regulated by N-Sst2 share common elements in the promoter region. This analysis revealed a CCCCT motif in 32 of the 40 genes (80%) induced by N-Sst2 (Table II). The CCCCT motif is a core consensus sequence of the stress response element (STRE), also known as a UAS_{PDS} (45–47). In addition, multiple copies of the motif were identified in 21 of the 40 N-Sst2-induced genes. In 15 of these genes, the CCCCT motifs were <60 bp apart. A similar analysis of the entire yeast genome revealed multiple copies of the motif in 515 of 6,144 genes (8.4%), 212 of which are within 60 bp of one another (3.4%). Previous gene profiling analysis has demonstrated that most genes induced upon treatment with NaCl contain the CCCCT sequence (48). The sequence CCCCT functions in both directions (49). Of the 32 genes identified here, the motif was found in both the sense (49%) and antisense (51%) orientations.

Microarray analysis provides a convenient measure of transcriptional regulation of a large number of genes. However, other methods are better suited to measure transcriptional regulation of specific genes, particularly under various physiological conditions or genetic backgrounds. To expand our analysis of N-Sst2 signaling, we turned to a reporter transcription assay composed of the *HSP12* promoter and *lacZ* (β-galactosidase) gene. This promoter was selected because the microarray data had indicated a substantial (8.6-fold) difference in *HSP12* transcript levels in cells that express N-Sst2 versus C-Sst2. Moreover, the promoter region of *HSP12* contains five STREs and has been previously used to monitor gene regulation in response to heat, high salt, and high osmolarity stress conditions (50).

We initially compared *HSP12-lacZ* induction in an *sst2*Δ

[2] P. Flanary and H. Dohlman, manuscript in preparation.

TABLE I

Microarray analysis of cells expressing N-Sst2 and C-Sst2

An *sst2*Δ mutant strain was transformed with plasmids containing either the N-Sst2 segment or the C-Sst2 segment, as described. Biotin-labeled cRNA was hybridized to a GeneChip set representing 6,412 genes and open reading frames. Units are RNA copies per million total transcripts. Gene descriptions are derived from YPD.

Qualifier	Gene names	N-SST2 copies	C-SST2 copies	-Fold change	YPD description
YMR105C	*PGM2*, *GAL5*	30	3	10	Phosphoglucomutase; major isozyme, interconverts Glc-1-P and Glc-6-P
YNL160W	*YGP1*	446	47	9.5	Secreted glycoprotein produced in response to nutrient limitation
YFL014W	*HSP12*, *GLP1*	95	11	8.6	Heat shock protein of 12 kDa, induced by heat, osmotic stress, oxidative stress and in stationary phase
YMR104C	*YPK2*, *YKR2*	43	5	8.6	Serine/threonine protein kinase with similarity to Ypk1p
YDR277C	*MTH1*, *BPC1*	57	7	8.1	Repressor of hexose transport genes
YEL011W	*GLC3*	81	10	8.1	α-1,4-Glucan branching enzyme (glycogen branching enzyme), necessary for glycogen synthesis
YFR053C	*HXK1*, *HKA*	338	43	7.9	Hexokinase I, converts hexoses to hexose phosphates in glycolysis; repressed by glucose
YMR081C	*ISF1*, *MBR3*	23	3	7.7	Protein that participates with Nam7p/Upf1p in suppression of mitochondrial splicing defect
YBR072W	*HSP26*	74	10	7.4	Heat shock protein of 26 kDa, expressed during entry to stationary phase and induced by osmostress
YER067W		172	24	7.2	Protein of unknown function
YER150W	*SPI1*	401	56	7.2	Protein induced in stationary phase, has similarity to Sed1p
YDR070C		63	9	7	Protein of unknown function
YER103W	*SSA4*	342	50	6.8	Protein chaperone of the HSP70 family, cytoplasmic heat-induced form that is not expressed under optimal conditions
YJL170C	*ASG7*	53	8	6.6	Protein expressed only in cells of mating type a, inhibits inappropriate pheromone response by regulation of Ste4p localization
YBR054W	*YRO2*	159	25	6.4	Protein paralog of Mrh1p, has similarity to heat shock protein Hsp30
YFR015C	*GSY1*	82	14	5.9	UDP-glucose-starch glucosyltransferase (glycogen synthetase) isoform 1
YEL039C	*CYC7*	35	6	5.8	Cytochrome *c* isoform 2, predominant isoform during anaerobic growth
YLR327C		168	29	5.8	Protein with strong similarity to Stf2p
YFR017C		95	17	5.6	Protein of unknown function
YOR161C		67	12	5.6	Protein of unknown function
YOL053C-A		421	83	5.1	
YHR087W		85	17	5	Protein of unknown function
YGR088W	*CTT1*	109	22	5	Catalase T (cytosolic), important for detoxification of superoxide radicals and hydrogen peroxide
YDR074W	*TPS2*, *HOG2*, *PFK3*	296	60	4.9	Trehalose-6-phosphate phosphatase, component of the trehalose-6-phosphatase synthase/phosphatase complex
YPR160W	*GPH1*	54	11	4.9	Glycogen phosphorylase, releases α-D-glucose-1-phosphate from glycogen complex
YAL061W	*FUN50*	48	10	4.8	Member of the zinc-containing alcohol dehydrogenase family, transcription is induced in response to PDR1 gain-of-function mutations
YGL117W		51	11	4.6	Protein of unknown function; transcription induced by the drug FK506 in a GCN4-dependent manner
YML128C	*MSC1*	55	12	4.6	Protein of unknown function that affects meiotic homologous chromatid recombination
YNL036W	*NCE103*, *NCE3*	242	55	4.4	Protein involved in protection against oxidative damage
YPL247C		110	25	4.4	Protein of unknown function, has WD (WD-40) repeats
YIL121W		26	6	4.3	Member of the multidrug resistance 12-spanner (DHA12) family of the major facilitator superfamily (MFS-MDR)
YDL214C	*PRR2*	51	12	4.3	Serine/threonine protein kinase potentially involved in pheromone response
YGR008C	*STF2*	97	23	4.2	ATPase-stabilizing factor, binds to F_0-ATPase; facilitates binding of inhibitor and 9-kDa protein to F_1-ATPase
YDR542W		268	64	4.2	Member of the seripauperin (PAU) family
YAL068C		284	68	4.2	Member of the seripauperin (PAU) family
YDL204W		25	6	4.2	Protein of unknown function
YLR149C		25	6	4.2	Protein of unknown function
YIL082W-A		393	95	4.1	
YKL148C	*SDH1*, *SDHA*, *HAR2*	41	10	4.1	Succinate dehydrogenase (ubiquinone) flavoprotein (Fp) subunit, converts succinate plus ubiquinone to fumarate plus ubiquinol in the tricarboxylic acid cycle
YHR092C	*HXT4*, *LGT1*, *RAG1*	61	15	4.1	Moderate to low affinity hexose transporter, member of the hexose transporter family of the major facilitator superfamily (MFS)
YLR452C	*SST2*	2	263	0	Regulator of G protein signaling family member that negatively regulates the mating pheromone response pathway by binding to Gpa1p and stimulating its intrinsic GTP
YMR058W	*FET3*	32	321	0.1	Cell surface ferroxidase; required for high affinity ferrous iron uptake
YEL065W	*SIT1*, *ARN3*	9	87	0.1	Ferrioxamine B permease, member of the yeast-specific multidrug resistance (MFS-MDR) family of the major facilitator superfamily (MFS)
YER145C	*FTR1*	12	98	0.1	Iron permease that mediates high affinity iron uptake
YLR237W	*THI7*, *THI10*, *UPL3*	30	220	0.1	Thiamine transport protein, member of the uracil/uridine/allantoin permease family of membrane transporters
YDR270w	*CCC2*	7	48	0.1	Copper-transporting P-type ATPase, member of the heavy metal transporting P-type ATPases in the superfamily of P-type ATPases
YDR094W		9	55	0.2	Protein of unknown function
YDR144C	*MKC7*, *YPS2*	18	98	0.2	Aspartyl protease found in the periplasmic space, has similarity to Yps1p and Bar1p
YPL282C	*YOR394W*	5	23	0.2	Member of the seripauperin (PAU) family (YPL282C and YOR394W code for identical proteins)
YDR120C	*TRM1*	25	114	0.2	N^2,N^2-dimethylguanine tRNA methyltransferase, required for methylation of G26 of both mitochondrial and cytoplasmic tRNAs
YDR209C		6	27	0.2	Protein of unknown function
YDR180W	*SCC2*	10	44	0.2	Cohesin, protein required for mitotic sister chromatid cohesion
YDL158C		5	22	0.2	Protein of unknown function
YDR372C		9	37	0.2	Protein of unknown function

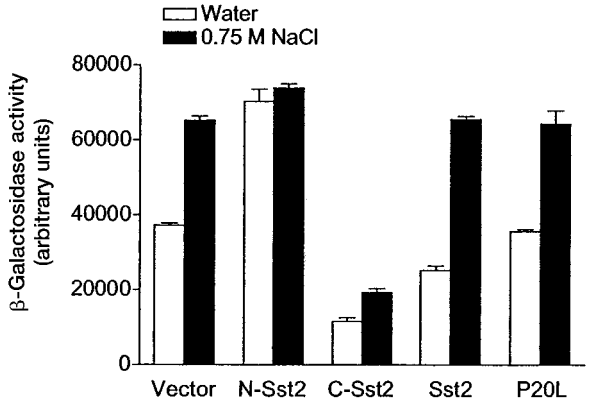

FIG. 1. **Stress-dependent reporter transcription assay: N-Sst2 *versus* C-Sst2.** An *sst2*Δ mutant strain (YDM400) was transformed with a plasmid containing the stress-activated *HSP12* promoter and *lacZ* reporter gene (pRS423-HSP12-*lacZ*) and a plasmid having no insert (*Vector*; pRS316-ADH), N-*SST2*, C-*SST2*, full-length *SST2*, or the *SST2*^{P20L} (*P20L*) mutant. Cells were grown to mid-log phase, treated with NaCl or water for 10 min, and assayed for β-galactosidase activity. Data shown are typical of three independent experiments performed in triplicate. *Error bars*, ±S.E.

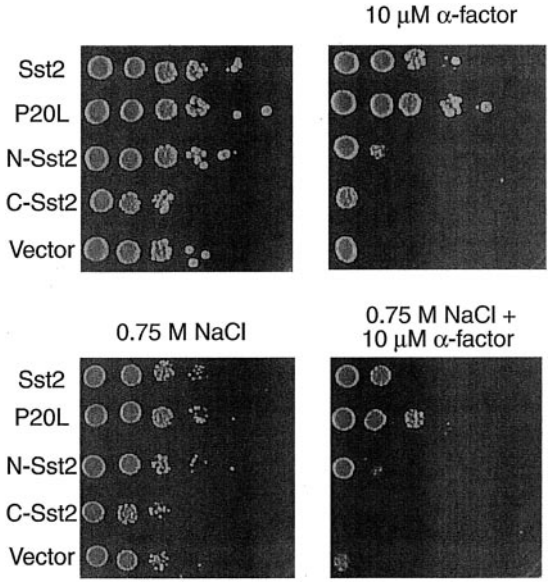

FIG. 2. **Stress-mediated growth inhibition: N-Sst2 versus C-Sst2.** An *sst2*Δ mutant strain (YDM400) was transformed with a plasmid containing full-length *SST2*, *SST2*^{P20L}, N-*SST2*, C-*SST2*, or no insert (*Vector*; pRS316-ADH). Cells were grown to saturation, diluted to $A_{600} \sim 0.2$, grown to $A_{600} \sim 0.8$, and then treated with 10 μM α-factor (final concentration) or water for 2 h. 10 μl of cells were spotted onto solid synthetic medium containing 0.75 M NaCl either without dilution or diluted 1:10, 1:100, 1:1,000, 1:10,000, and 1:100,000 with water or with 10 μM α-factor (as indicated). Resulting growth was documented after 24 h.

TABLE II

Genes induced by N-Sst2 contain a stress-response element

Alignace was used to identify motifs of 8 nucleotides in length within the 5′ intergenic region of each open reading frame. Genespring was used to search for highly conserved sequence elements, and for statistical analysis. The Transfac database was used to identify potential transcription factor binding sites. Starting positions of the CCCCT and CCCCTTAT motifs are provided, relative to the initiator ATG. N/C, ratios of transcript numbers for N-Sst2 and C-Sst2.

Qualifier (gene names)	N/C	Location of CCCCT	CCCCTTAT
YMR105C (*PGM2*, *GAL5*)	10.0	216, 259, 305, 359, 406	
YNL160W (*YGP1*)	9.5	434	
YFL014W (*HSP12*, *GLP1*)	8.6	190, 232, 377, 414, 435	
YDR277C (*MTH1*)	8.1	319	319
YEL011W (*GLC3*)	8.1	213, 282, 374	
YFR053C (*HXK1*)	7.9	337, 478	
YBR072W (*HSP26*)	7.4	326, 461, 479	326
YER150W (*SPI1*)	7.2	258, 265, 373	
YER0676W	7.2	218, 234, 279, 409	
YDR070C	7.0	201	
YER103W (*SSA4*)	6.8	179, 432, 467	
YFR015C (*GSY1*)	5.9	332, 467	
YEL039C (*CYC7*)	5.8	192, 276, 336	336
YLR327C	5.8	337	
YFR017C	5.6	238, 264	
YOR161C	5.6	281, 290	
YOL053C-A	5.1	175, 203, 248, 472	175
YGR088W (*CTT1*)	5.0	101, 331, 346	
YHR087W	5.0	200, 302, 483	200
YPR160W (*GPH1*)	4.9	308, 357	
YDR074W (*TPS2*, *HOG2*, *PFK3*)	4.9	326, 421, 441, 490	
YAL061W (*FUN50*)	4.8	262, 312	
YML128C (*MSC1*)	4.6	132, 202	
YNL036W (*NCE103*, *NCE3*)	4.4	189	
YPL247C	4.4	144, 151	
YDL214C (*PRR2*)	4.3	441, 477	
YGR008C (*STF2*)	4.2	188, 279	
YDR542W	4.2	328	
YAL068C	4.2	326	
YDL204W	4.2	160	160
YLR149C	4.2	159, 461	162
YKL148C (*SDH1*, *HAR2*)	4.1	80	80

strain transformed with either N-Sst2, C-Sst2, full-length Sst2, or the empty vector (no Sst2 expressed). In addition, we tested a gain-of-function allele, *SST2*^{P20L}. This mutation confers dominant pheromone resistance, through an as yet uncharacterized mechanism (51). As shown in Fig. 1, there was a 6-fold difference in activity in cells expressing N-Sst2 versus C-Sst2 (70,302 and 11,613 units of activity, respectively). Full-length Sst2 yielded an intermediate level of activity (25,209 units), slightly below that of cells lacking Sst2 (empty vector, 37,156 units). The Sst2^{P20L} mutant behaved like the vector control. Thus, the results of the reporter transcription assay corroborate the differences observed by microarray analysis, in which the basal level of expression was highest for N-Sst2 and lowest for C-Sst2. An intermediate basal activity was observed for full-length Sst2 (Fig. 1).

We then examined if N-Sst2 could modulate *HSP12-lacZ* induction by exposure to high concentrations of salt (0.75 M NaCl), a known activator of the stress response pathway. As shown in Fig. 1, there was minimal salt induction of *HSP12-lacZ* in cells expressing N-Sst2. In contrast, there was a larger induction in cells expressing full-length Sst2 (2.6-fold), C-Sst2 (1.7-fold), or no Sst2 (vector control, 1.8-fold) (Fig. 1). These data indicate that N-Sst2 is a potent activator of the stress response pathway, but the high basal activity leads to a diminished salt induction.

High concentrations of NaCl are known to inhibit cell growth, in addition to stimulating expression of STREs. Moreover, a number of mutants with disrupted signaling to STRE genes will grow poorly in high osmolarity medium (50). Thus, we examined whether N-Sst2 (or C-Sst2) has any effect on growth in high salt. Saturated cultures were diluted and spotted onto solid medium, either in the absence or presence of 0.75 M NaCl. In the absence of salt, cells expressing full-length Sst2, N-Sst2, or vector grew equally well (Fig. 2, *top left panel*). The growth of these strains was impaired to a similar extent in salt-containing medium (Fig. 2, *bottom left panel*). In contrast, cells expressing C-Sst2 grew more poorly than the other transformed strains, in the absence or presence of salt. These results parallel the *HSP12-lacZ* reporter transcription data presented in Fig. 1. Since the C-Sst2-containing cells are unable to ex-

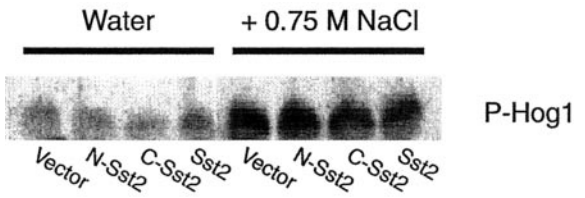

FIG. 3. **Stress-mediated Hog1 phosphorylation: N-Sst2 *versus* C-Sst2.** An *sst2*Δ mutant strain (YDM400) was transformed with a plasmid containing no insert (*Vector*; pRS316-ADH), N-*SST2*, C-*SST2*, or full-length *SST2*. Cells were grown to mid-log phase and treated with NaCl or water for 60 min. Cell lysates were prepared and subjected to 8% SDS-PAGE and immunoblotting with anti-phosphotyrosine antibodies to detect phosphorylated-Hog1 (*P-Hog1*).

press normal amounts of an STRE-containing gene, they are evidently unable to mount a full response to stress growth conditions. Even in normal medium, the growth of the C-Sst2 cells is impaired, as if they were exposed to salt. Conversely, N-Sst2 expression mimics the transcriptional induction observed with salt treatment, and these cells are able to grow well in the absence or presence of high salt concentrations.

We then examined if pheromone treatment would alter the growth of cells expressing N-Sst2 or C-Sst2, in the absence or presence of salt. Pheromone is known to impair growth, leading to cell cycle arrest in G_1. Cells lacking *SST2* are supersensitive to pheromone-induced growth arrest. However, we have previously shown that neither N-Sst2 nor C-Sst2 alone can rescue an *sst2*Δ mutation (18). Consistent with these earlier observations, cells expressing N-Sst2, C-Sst2, or vector grew poorly in the presence of pheromone, compared with the full-length protein (Fig. 2, *top right panel*). Pheromone-treated cells expressing the gain-of-function mutant $Sst2^{P20L}$ grew better than those with full-length Sst2, as previously reported (51). Cells expressing C-Sst2 grew poorly in the presence or absence of high salt, and even more poorly in the presence of salt plus pheromone (Fig. 2, *bottom right panel*). This pattern of additive growth inhibition was evident throughout and is consistent with separate and additive mechanisms of action.

Genetic studies have revealed at least two osmosensing pathways that converge on the MAP kinase kinase Pbs2, leading to tyrosine phosphorylation of the MAP kinase Hog1 (52). MAP kinases are the only tyrosine-phosphorylated proteins in yeast, and Hog1 is the only MAP kinase phosphorylated in response to salt stress (52). Thus, we examined if N-Sst2 or C-Sst2 have any effect on Hog1 phosphorylation, by immunoblotting whole cell extracts with anti-phosphotyrosine antibodies. As shown previously (52), salt treatment leads to a dramatic increase in Hog1 phosphorylation (Fig. 3). However, Hog1 phosphorylation is largely unaffected by expression of N-Sst2 or C-Sst2, in the absence or presence of added salt. These results are in contrast to the reporter transcription assay presented above, in which N-Sst2 stimulated, and C-Sst2 inhibited, basal expression of *HSP12-lacZ*. These data together with those presented in Fig. 2 suggest that N-Sst2 acts through another, Hog1-independent, pathway.

One way to determine the biological role of N-Sst2 is through the identification of associated proteins. To this end, we carried out a two-hybrid screen against an array of nearly all yeast open reading frames. A strain expressing N-Sst2 fused to the Gal4 DNA-binding domain was mated to a set of ~6,000 colonies, each expressing a unique full length open reading frame fused to the Gal4 activation domain. Any proteins identified in two independent screens were analyzed further. As shown in Table III, N-Sst2 reproducibly yielded 17 putative interactions. This compares to an average of 3.3 positives per protein obtained for an independent set of 192 DNA binding domain hybrids, described previously (20). Using an identical screening array, full-length Sst2 yielded no specific positives. Mpt5, a protein shown to bind Sst2 in a previous two-hybrid screen, was not identified in our screen. Genetic analysis revealed that Mpt5 can attenuate pheromone signaling downstream of the G protein and independently of the C-terminal RGS domain (53, 54).

Of the 17 putative N-Sst2-binding proteins, five (29%) were listed by the Yeast Protein Data base as unclassified, having no known functional or structural homologues. This value is similar to the percentage of unclassified genes listed throughout the entire data base. At least three of these genes, *PEP12*, *TLG2*, and *VPS36*, are required for proper sorting of vacuolar proteases and normal vacuolar morphology (55–64). Several other interacting proteins are protein kinases, including Iks1, and a member of the MAP kinase family Kss1 (*KSS1* product, kinase suppressor of *sst2*). Kss1 can phosphorylate Sst2 at Ser^{539}, which is located in the C-terminal domain of the protein (65).

We then examined whether any of the potential N-Sst2 binding partners are required to transmit a signal via the stress response pathway. Gene deletion mutants were obtained for 15 of the 17 interacting proteins and evaluated for changes in *HSP12-lacZ* activity. As shown in Fig. 4, all three of the vacuolar sorting mutants, *pep12*Δ, *tlg2*Δ, and *vps36*Δ, yielded a high basal activity. In addition, these mutants exhibited a diminished induction with salt treatment (1.4-, 1.8-, and 2.1-fold, respectively) as compared with the wild-type strain (2.6-fold induction). This pattern of activity (high basal, low induction) resembles that seen with N-Sst2 in Fig. 1. Our positive control for this assay was a deletion of the high osmolarity glycerol kinase gene *HOG1* (52). Like N-Sst2 and the binding partner mutants, the *hog1*Δ strain exhibited a diminished induction with salt (2.1-fold). In contrast to the other mutants, however, *hog1*Δ exhibited a normal or slightly reduced basal activity. We also tested four other vacuolar sorting mutants, *vps5*Δ, *vps20*Δ, *vps21*Δ, and *vps25*Δ. Vps5 was chosen because it contains a phosphoinositide-binding Phox homology (PX) domain, which is found in the mammalian RGS protein RGS-PX1 (66). Vps20 and Vps25 were reported previously to interact with Vps36 in two-hybrid assays (20, 21). Vps21 was chosen arbitrarily as a negative control to rule out the possibility that altered STRE signaling is a generalized consequence of impaired vacuolar function. As shown in Fig. 4, all four mutants exhibited normal basal and salt-induced activities. Taken together, these data indicate that *PEP12*, *TLG2*, and *VPS36* are necessary for full activation of the stress response pathway but act in a manner distinct from the well characterized Hog1 kinase.

Sst2 is well known to regulate pheromone signaling. An *sst2*Δ mutant can enhance pheromone sensitivity by >100-fold. Thus, we then examined if any of the 15 candidate binding partners could also regulate the pheromone response. For these experiments, two standard bioassays were used. In the halo assay, cells are spread onto solid media and exposed to α-factor pheromone spotted onto filter disks. The resulting zone of growth inhibition gives an indication of pheromone response (halo size) and recovery (halo turbidity). Of the 15 mutants tested, only *vps36*Δ, *pep12*Δ, and *tlg2*Δ produced more turbid zones of growth inhibition, as compared with the wild-type control, indicating an enhanced ability to recover from pheromone-induced growth arrest. An additional mutant (*kel1*Δ) had the opposite effect, producing halos that were slightly larger and less turbid than the wild-type control (Fig. 5*A*).

A number of vacuolar sorting mutants have previously been reported to produce turbid halos (67). Halo turbidity in the vacuolar sorting mutants could result from missorting and

TABLE III

Genome-wide two-hybrid analysis using N-Sst2 as bait

A strain expressing N-Sst2 fused to the Gal4 DNA-binding domain was mated to a set of ~6,000 colonies, each expressing a unique full-length open reading frame fused to the Gal4 activation domain, as described. Proteins identified in two independent screens with the same bait are listed. Only genes identified in 10 or fewer screens are listed, since those identified at a higher frequency are likely to be nonspecific ("false") positives. Functional descriptions and number of amino acids (aa) are from the YPD database (note that *MVP1* is erroneously listed in YPD as being required for vacuolar protein sorting). Predicted conserved sequence motifs are from the SMART data base (16, 93). TM, transmembrane domain, S/TK, serine/threonine protein kinases catalytic domain. CC, coiled-coil domain. SH3, Src homology 3 domain. FH2, formin homology 2 domain. ZnF RBZ, zinc finger Ran-binding domain. RING, ring finger domain with possible ubiquitin-protein ligase activity. PX, PhoX homologous domain. tSNARE, helical region found in SNAREs. SynN, syntaxin N-terminal domain.

Qualifier (gene names)	YPD description
YDL180W	Protein of unknown function, 547 aa, 7 TM
YDL186W	Protein of unknown function, 277 aa,
YDR319C	Protein of unknown function, 274 aa, 6 TM
YER118C (*SHO1*, *SSU81*)	Osmosensor in the HOG1 MAP kinase, high osmolarity signal transduction pathway, has an SH3 domain, 367 aa, 4 TM, 1 SH3
YER188W	Protein of unknown function, 239 aa
YGR040W (*KSS1*)	Serine/threonine protein kinase involved in the filamentous and invasive growth pathway, member of the MAP kinase family, 368 aa, S/TK
YGR018C	Protein of unknown function, 109 aa
YGR172C (*YIP1*)	Protein involved in vesicular transport; interacts with transport GTPases Ypt1p and Ypt31p at the Golgi membrane, 248 aa, 5 TM
YHR158C (*KEL1*)	Protein involved in cell fusion and morphology, contains six Kelch repeats, 1164 aa, 3 CC
YIL159W (*BNR1*)	Bni1p-related protein, potential target of Rho4p, 1375 aa, 1 CC, 1 FH2
YJL057C (*IKS1*)	Probable serine/threonine protein kinase, 667 aa, S/TK
YLR417W (*VPS36*, *VPL11*, *GRD12*, *VAC3*)	Protein involved in vacuolar sorting; mutant displays a prominent novel prevacuolar organelle, 566 aa, 2 ZnF RBZ, possible RING
YLR457C (*NBP1*)	Essential protein required for G_2/M transition, 319 aa, 1 CC
YML038C (*YMD8*)	Member of the triosephosphate translocater family of membrane transporters, has weak similarity to Gog5p vanadate resistance protein, 442 aa, 9 TM
YMR004W (*MVP1*)	Protein required for sorting proteins to the vacuole, interacts genetically with Vps1p, 511 aa, 1 PX
YOL018C (*TLG2*)	Syntaxin homolog (t-SNARE), involved in efficient endocytosis and in maintenance of resident proteins in the trans-Golgi network, 397 aa, 1 tSNARE, 1 TM
YOR036W (*PEP12*, *VPL6*, *VPT13*, *VPS6*)	Syntaxin homolog (t-SNARE) involved in Golgi to vacuole transport, 288 aa, 1 SynN, 1 tSNARE, 1 TM

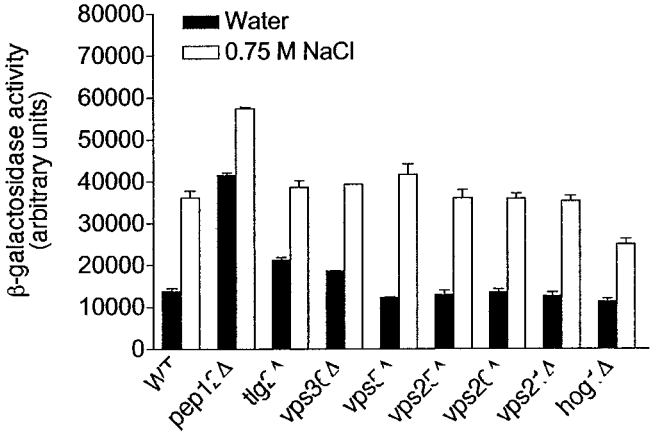

FIG. 4. **Loss of N-Sst2-binding proteins induces a stress-activated promoter.** Wild-type and gene disruption mutants were transformed with a plasmid containing the stress-activated *HSP12* promoter and *lacZ* reporter gene (pRS423-HSP12-lacZ). Cells were grown to mid-log phase and treated with 0.75 M NaCl or water for 10 min, and the resulting β-galactosidase activity was measured as described under "Experimental Procedures." Data shown are typical of three independent experiments performed in triplicate. *Error bars*, ±S.E.

secretion of vacuolar proteases and the consequent proteolysis of pheromone or the pheromone receptors. Indeed, we found that each of the *vps* mutants tested (*vps5*Δ, *vps20*Δ, *vps21*Δ, *vps25*Δ, *vps35*Δ, *vps38*Δ) also yielded slightly turbid halos (data not shown). To provide an independent assessment of pheromone sensitivity, we tested each of the candidate binding partners using a pheromone-responsive transcription reporter assay (*FUS1* promoter, *lacZ* reporter). In agreement with the results of the halo assay, *vps36*Δ, *pep12*Δ, and *tlg2*Δ exhibited a diminished transcription response (Fig. 5*B*, *top panel*). The effects were particularly dramatic for the *vps36*Δ and *tlg2*Δ mutants, with reductions of 30 and 50%, respectively. Deletion of two candidate Vps36-binding partners (*vps20*Δ, *vps25*Δ) also resulted in a diminished response, equal to or greater than that exhibited by *vps36*Δ (Fig. 5*B*, middle). One of the control mutants (*vps5*Δ) responded like wild-type, while a second (*vps21*Δ) had a diminished response. Therefore, two additional control mutants (*vps35*Δ and *vps38*Δ, selected arbitrarily) were tested and found to also respond like wild-type (Fig. 5*B*, *bottom*). Thus, in addition to their role in stress response signaling, *VPS36*, *TLG2*, and *PEP12* are also necessary for full activation of the pheromone response pathway. The pheromone signaling phenotype is seen with some but not all *vps* mutants. The stress signaling phenotype is not shared by any of the other *vps* mutants. Taken together, these data indicate that Vps36, Tlg2, and Pep12 function in a manner similar to N-Sst2 but distinct from other vacuolar sorting factors.

Because it has an especially strong pheromone signaling phenotype and because it has not been well characterized previously, we selected Vps36 for further analysis. We first showed that a plasmid-borne copy of Vps36 could reverse the pheromone-resistant phenotype of the *vps36*Δ mutation (Fig. 6*A*). Overexpression of Vps36 in a wild-type strain did not further enhance signaling and even had a modest inhibitory effect (Fig. 6, *A* and *B*). However, overexpression of Vps36 in cells lacking *SST2* did result in a dramatic elevation of pheromone sensitivity (Fig. 6*B*). The signal-enhancing effects of Vps36 may be unmasked when Sst2 protein levels are low, as occurs in the absence of pheromone (30).

Having shown that Vps36 activity is diminished by Sst2, we next examined whether Sst2 activity is similarly dependent on Vps36. Overexpression of full-length *SST2* is well known to inhibit the pheromone response (30). Overexpression of Sst2 also reduces the already diminished response of the *vps36*Δ strain (Fig. 7), indicating that Sst2 can inhibit signaling in the absence of Vps36. In contrast, overexpression of N-Sst2 has no

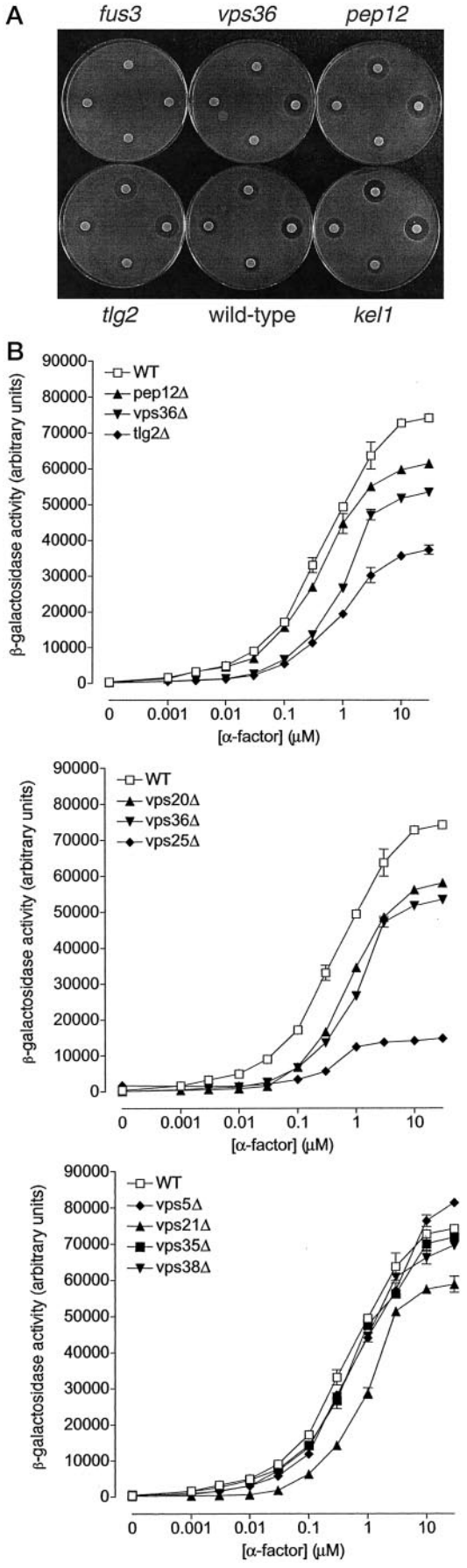

FIG. 5. **Loss of N-Sst2-binding proteins inhibits the pheromone response pathway.** *A*, wild-type and mutant strains were plated, and the nascent lawn was exposed to sterile filter discs spotted with α-factor (from *bottom clockwise*: 15, 25, 50, and 75 μg for 48 h) and then photographed. The wild-type strain BY4741 is a negative control, and the isogenic *fus3*Δ strains are a positive control. Other mutants tested but not shown (*vps5*Δ, *vps20*Δ, *vps21*Δ, *vps25*Δ, *vps35*Δ, and *vps38*Δ) also produced slightly turbid halos. *B*, wild-type and mutant strains were transformed with a plasmid containing the pheromone-responsive *FUS1* promoter-*lacZ* reporter. Cells were then treated with the indicated concentrations of α-factor, and the resulting β-galactosidase activity was measured as described under "Experimental Procedures." Data shown are typical of three independent experiments performed in triplicate. *Error bars*, ±S.E.

effect on signaling in a wild-type strain (Fig. 2) (18). Presumably, this is because N-Sst2 lacks the GTPase accelerating activity associated with the C-terminal RGS domain. Remarkably, N-Sst2 is a potent inhibitor in the *vps36*Δ mutant and is even more active than full-length Sst2 (Fig. 7). Thus, a signal-dampening effect of Sst2 is unmasked when Vps36 is absent, and this effect resides in the N-Sst2 domain. These data suggest an *antagonistic* relationship between Vps36 and Sst2, in their ability to regulate the pheromone response pathway.

Sst2 is well known to attenuate signaling through its ability to accelerate Gα GTPase activity. Thus, we examined whether Vps36 also acts through the G protein α subunit or if it affects signaling downstream of the G protein. Gα-independent signaling was achieved through overexpression of *STE4* (Gβ), mutational activation of *STE11* (effector kinase), and overexpression of *STE12* (transcription factor). Overexpression of *STE4* results in elevated levels of the Gβγ complex, above that which can bind to Gα (68–70). The *STE11*-4 mutant encodes a constitutively active form of the mitogen-activated protein kinase kinase kinase, *Ste11* (34). Overexpression of *STE12* results in elevated transcription of PRE-containing genes (71). As shown in Fig. 8, the *vps36*Δ mutant attenuated signaling by at least 25% in every case, whether or not α-factor was added. These data suggest that Vps36 can function downstream of the G protein, independently of Sst2 RGS activity, and most likely at the level of transcription.

DISCUSSION

The GTPase accelerating activity of RGS proteins is well established. However, many RGS family members are likely to have other functions as well. Our goal was to identify a possible signaling function for the N-terminal (non-RGS-homologous) domain of Sst2. Yeast has specific advantages for this type of investigation, since nearly every gene has been arrayed for RNA expression studies, subjected to two-hybrid analysis, and genetically disrupted. Here, a comprehensive analysis of transcription indicates that N-Sst2 regulates a pathway leading to STRE activation. Comprehensive two-hybrid analysis has revealed candidate targets of N-Sst2 action. The functional significance of some of these interactions was established using gene disruption mutations, in conjunction with functional assays of stress- and pheromone-mediated signaling in yeast. Of the 17 proteins identified as potential N-Sst2 interactors, at least one has previously been implicated in STRE activation. Sho1 is thought to act by recruiting the MAP kinase kinase Pbs2 to the plasma membrane (72–74). Pbs2 phosphorylates Hog1, which in turn activates the transcription factors Msn2 and Msn4 (48, 75). Msn2/4 are known to bind to the CCCCT motif present in stress-activated genes (46, 47, 76, 77). Not surprisingly, deletion of *MSN2* and *MSN4* results in poor growth and decreased induction of STRE-regulated genes upon exposure to high osmolarity media, heat shock, nutrient limitation, and oxidative stresses (46, 47, 77). However, our analysis indicates that binding of N-Sst2 to Sho1 is of little functional consequence, at least with respect to Hog1 phosphorylation (Fig. 3). Moreover, the pattern of *HSP12-lacZ*

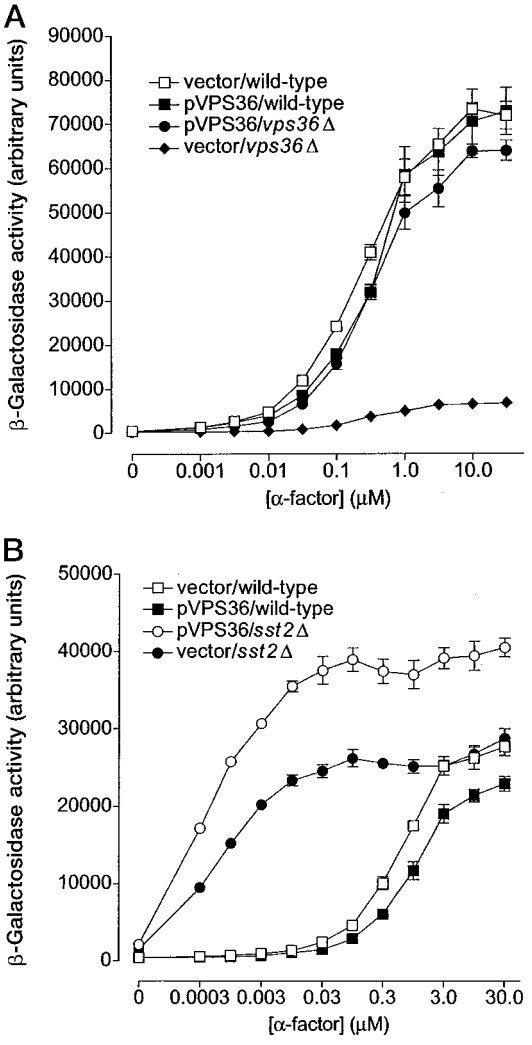

FIG. 6. **Overexpression of VPS36 enhances pheromone response signaling.** Wild-type, *vps36*Δ (*A*), and *sst2*Δ (*B*) cells were transformed with a plasmid containing the *FUS1-lacZ* reporter and a plasmid (pYES2.1/V5-His-TOPO) containing either no insert (*vector*) or *VPS36* (pVPS36). Cells were treated with the indicated concentrations of α-factor, and the resulting β-galactosidase activity was measured as detailed under "Experimental Procedures." A greater loss of signaling was observed in this experiment as compared with Fig. 5, evidently due to the use of galactose-containing media. Data shown are typical of three independent experiments performed in quadruplicate. *Error bars*, ±S.E.

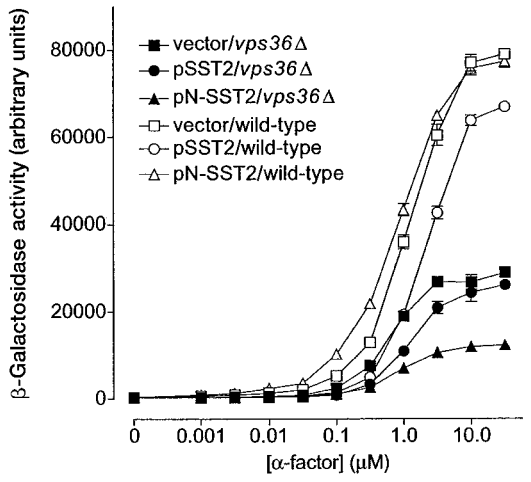

FIG. 7. **Loss of Vps36 enhances the activity of N-Sst2.** Wild-type and *vps36*Δ cells were transformed with a plasmid containing the *FUS1-lacZ* reporter and a plasmid (pYES2.1/V5-His-TOPO) containing either no insert (*vector*), N-*SST2* (pN-SST2), or full-length *SST2* (pSST2). Cells were treated with the indicated concentrations of α-factor, and β-galactosidase activity was determined as detailed under "Experimental Procedures." Data shown are typical of three independent experiments performed in quadruplicate. *Error bars*, ± S.E.

activation by N-Sst2 resembles that of the N-Sst2 binding partner mutants (high basal, low salt induction) (Fig. 1) but is substantially different from that of the *hog1*Δ mutant (normal basal, low salt induction) (Fig. 4).

Another pathway suggested to contribute to the stress response involves Gpa2 (the only other G protein in yeast besides Gpa1) (78). Gpa2 is activated by a putative glucose receptor, Gpr1, and transmits a signal leading to activation of adenylyl cyclase and the cAMP-dependent protein kinase. Gene profiling studies have been conducted following activation of the cAMP-cAMP-dependent protein kinase pathway (79) and have revealed 17 genes that are repressed by cAMP, 10 of which are dependent on *MSN2* and *MSN4* expression. We noted that eight of the cAMP-regulated genes show at least a modest increase in cells expressing N-Sst2, and two of these increase by at least 2-fold: *YAK1* (YJL141C) and YHR033. In comparison, over half the genes induced by N-Sst2 were previously identified as being induced after a shift to high osmolarity medium (48). Our data suggest that STREs may be activated by a distinct signaling pathway that is dependent on N-Sst2. Whole genome two-hybrid analysis revealed three components that also modulate transcription of an STRE-containing gene. Prior data have indicated that all three proteins are necessary for different aspects of protein trafficking and vacuolar function in yeast cells. Tlg2 is a syntaxin (t-SNARE) that functions in transport from the endosome to the late Golgi within the endocytic pathway (55, 56). Pep12 is a syntaxin that is required for protein sorting between the Golgi and endosome (57, 58). Vps36 is one of a diverse class of gene products needed for protein trafficking from the pre-vacuolar compartment to the vacuole (59–62). Notably, an earlier screen yielded a number of mutants with altered vacuolar function *and* diminished growth in high salt (63, 64). We have observed that this salt-sensitive growth phenotype is shared by the *vps36*Δ, *tlg2*Δ, and *pep12*Δ mutants (data not shown). This could result from altered signaling to STREs or more likely from defects in the transport of proteins that mediate osmotic regulation. STRE activation is not a general phenotype of vacuolar sorting mutants, however (Fig. 4).

An important question is whether the Vps36, Tlg2, and Pep12 bind physically to N-Sst2 or if they exert their documented *functional* effects through some common bridging protein. So far, direct binding of N-Sst2 to Vps36 and Tlg2 has been demonstrated using synthetic peptide arrays (80).[3] This analysis revealed binding to three discontinuous peptide "epitopes" within Vps36 and a single segment within Tlg2. This approach is also currently being used to identify the epitope(s) within N-Sst2 recognized by Vps36 and Tlg2.

Another significant question is whether Sst2 (like its putative binding partners) participates in protein sorting. This seems likely, since there is already considerable evidence that RGS proteins can regulate vesicle-mediated trafficking processes in other organisms. The mammalian RGS protein GAIP is associated with endoplasmic reticulum, Golgi, newly budded Golgi vesicles, and clathrin-coated vesicles (81, 82). GAIP appears to regulate secretion in epithelial cell lines (83) and lysosomal-autophagic catabolism in human colon cancer cells (84). Very recently, Farquhar and colleagues have described a

[3] P. Uetz, manuscript in preparation.

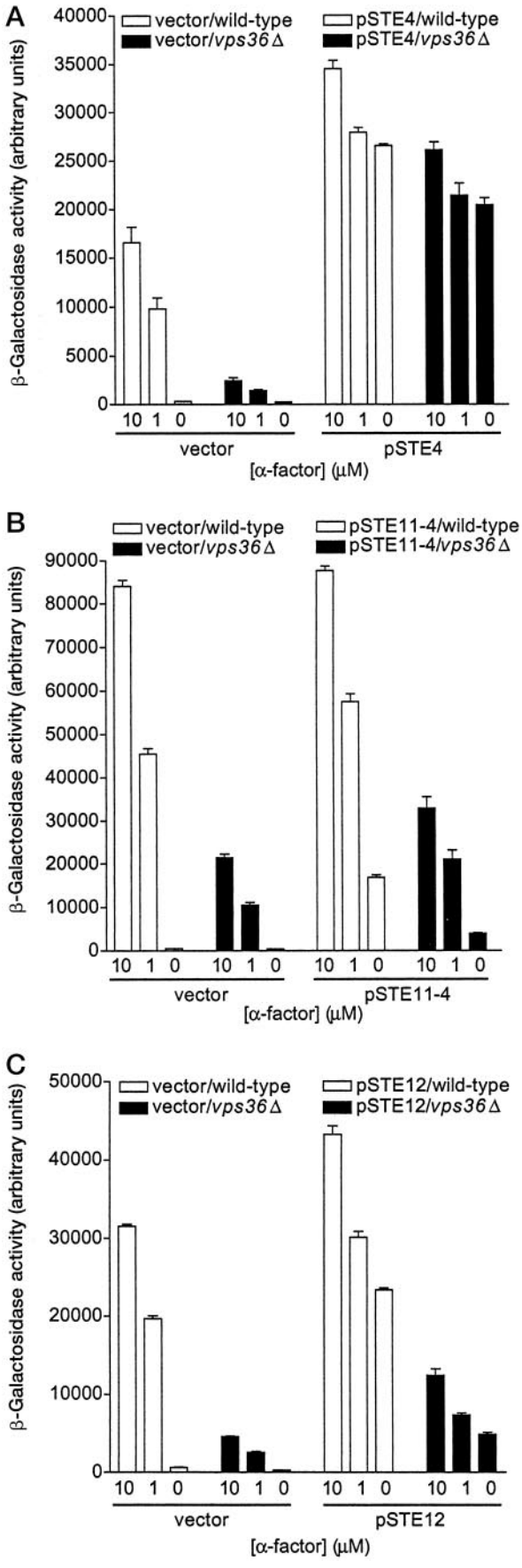

FIG. 8. **Vps36 acts late in the pathway.** Wild-type and *vps36*Δ cells were transformed with a plasmid containing the *FUS1-lacZ* reporter and a plasmid containing no insert (*vector*) or a plasmid that confers overexpression of Gβ (pSTE4) (*A*), expression of activated allele of Ste11 (pSTE11–4) (*B*), or overexpression of the transcription factor Ste12 (pSTE12) (*C*). Cells were treated with the indicated concentration of α-factor, and the resulting β-galactosidase activity was measured as detailed under "Experimental Procedures." Data shown are typical of three independent experiments performed in quadruplicate. *Error bars*, ±S.E.

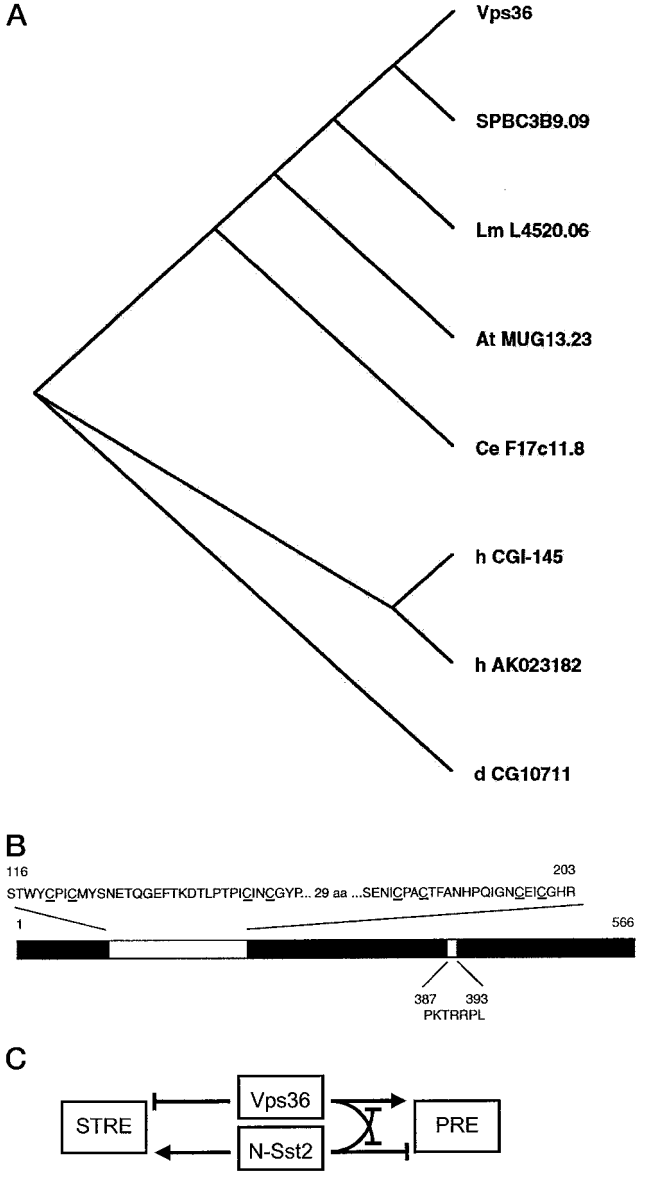

FIG. 9. **Vps36 and its homologues.** *A*, rectangular cladogram of Vps36 homologues. Some homologues to Vps36 were identified using advanced BLAST. Using an *E* value threshold of 0.01, PSI-BLAST revealed additional Vps36 homologues: CGI-145 (EAP45; $E = 1 \times 10^{-59}$), AK023082 ($E = 5 \times 10^{-57}$), and MUG13.23 ($E = 3 \times 10^{-58}$), all with two iterations. A third iteration identified L4520.06 ($E = 6 \times 10^{-6}$). Additional iterations produced no further sequence hits, demonstrating convergence. *SP*, *S. pombe*; *Lm*, *Leishmania major*; *At*, *Arabadopsis thaliania*; *Ce*, *C. elegans*; *h*, *Homo sapiens*; *d*, *Drosophila melanogaster*. *B*, Vps36 has two RBZ zinc binding Ran-GDP binding domains (*above left*, $E = 0.65$; *above right*, $E = 1.9 \times 10^{-4}$) with conserved Cys residues (*underlined*) as well as a nuclear localization signal of the pattern-7 type (*below*). *C*, *schematic diagram* summarizing the observed effects of Vps36 and N-Sst2 in STRE-*lacZ* and PRE-*lacZ* reporter assays. *Arrow*, stimulator; *bar*, inhibitor.

new protein called RGS-PX1, which contains an RGS domain as well as a PX domain similar to those in sorting nexin proteins (66). PX domains appear to help proteins reach their appropriate intracellular location through direct binding of

membrane-restricted phosphoinositides (85). In this regard, sorting nexins interact directly with endocytosed receptors, such as receptor tyrosine kinases activated by epidermal growth factor, but also have more general effects on endosomal traffic. RGS-PX1 was shown to accelerate GTP hydrolysis and inhibit signaling by $G_s\alpha$ and also to delay lysosomal degradation and inactivation of the epidermal growth factor receptor (66). Because of its bifunctional role as both a GTPase-accelerating protein and as a sorting nexin, RGS-PX1 may link heterotrimeric G protein signaling and vesicular trafficking in mammals. Sst2 might similarly link G protein signaling and vacuolar sorting in yeast. Sst2 is expressed only in haploid cells, however, so any membrane trafficking function would probably occur only in conjunction with mating. Another possibility is that Sst2 and Vps36 regulate transcription. Recently, Vps36 was reported to bind to Snf8, Vps25 (Yjr102), and Vps20 (20, 21). The human RNA polymerase II elongation factor-associated proteins EAP45 (or CGI-145, Fig. 9*A*), EAP30, and EAP20 appear to be homologous with Vps36, Snf8, and Vps25, respectively. The human EAPs form a complex that can inhibit elongation factor repression of RNA polymerase II activity (86–88). Likewise, a similar complex of Vps36, Snf8, and Vps25 might derepress RNA polymerase II in yeast. This could explain the absence of *SUC2* derepression in *snf8*Δ, *vps36*Δ, and *vps25*Δ mutants (86, 89). It could also explain how *VPS36* can coordinately regulate vacuolar trafficking and pheromone signaling. Vps36 must regulate STRE transcription by a distinct pathway, however, since the effects on this promoter occur independently of putative binding partners Vps25 and Vps20. Snf8 was not tested because of technical difficulties with the reporter transcription assay in the available knockout strain. Thus, our genetic analysis in yeast and parallel studies in human cells suggest that Vps36 acts at the level of transcription. Notably, we have identified a simple pattern-7 nuclear localization signal (*NLS*; Fig. 9*B*) and two novel zinc finger Ran-GDP binding domains (RBZ domain; Fig. 9*B*). Residues 120–186 could also form a RING finger domain, which is a specialized type of zinc finger involved in protein-protein interactions, including binding to E2 ubiquitin-conjugating enzymes (90). The RBZ domain may serve to recruit Vps36 to Ran-GDP. RanGDP is found nearly exclusively in the cytoplasm and the cytoplasmic face of the nuclear pore complex (91). The nuclear localization signal suggests that Vps36 may exist in the nucleus or shuttle between the cytoplasm and nucleus via the nuclear pore complex (92). However, while the RBZs and nuclear localization signal are present within the *S. cerevisiae* and *Schizosaccharomyces pombe* proteins, they are absent from Vps36 homologues in higher organisms (see Fig. 9*A*; data not shown).

In conclusion, Sst2 is one of a growing list of RGS proteins with at least two signaling functions. We have shown that Vps36 and the N-Sst2 domain can cooperatively regulate both the pheromone and stress response pathways. Whereas the pheromone response is inhibited by N-Sst2 and activated by Vps36, the stress response is activated by N-Sst2 and inhibited by Vps36 (Fig. 9*C*). The identification of candidate N-Sst2 binding proteins and their demonstrated role in stress signaling will be extremely useful in addressing the mechanism by which these proteins function within the cell. The approach used here also serves as a model for an integrated analysis of signaling pathways in other systems. Such an approach will be important for the identification and characterization of a large number of unknown gene products as they are identified through genome sequencing programs.

REFERENCES

1. Dohlman, H. G., and Thorner, J. W. (2001) *Annu. Rev. Biochem.* **70,** 703–754
2. Burchett, S. A. (2000) *J. Neurochem.* **75,** 1335–1351
3. Popov, S., Yu, K., Kozasa, T., and Wilkie, T. M. (1997) *Proc. Natl. Acad. Sci. U. S. A.* **94,** 7216–7220
4. Snow, B. E., Krumins, A. M., Brothers, G. M., Lee, S. F., Wall, M. A., Chung, S., Mangion, J., Arya, S., Gilman, A. G., and Siderovski, D. P. (1998) *Proc. Natl. Acad. Sci. U. S. A.* **95,** 13307–13312
5. Siderovski, D. P., Diverse-Pierluissi, M., and De Vries, L. (1999) *Trends Biochem. Sci.* **24,** 340–341
6. Cabrera, J. L., de Freitas, F., Satpaev, D. K., and Slepak, V. Z. (1998) *Biochem. Biophys. Res. Commun.* **249,** 898–902
7. Kim, E., Arnould, T., Sellin, L., Benzing, T., Comella, N., Kocher, O., Tsiokas, L., Sukhatme, V. P., and Walz, G. (1999) *Proc. Natl. Acad. Sci. U. S. A.* **96,** 6371–6376
8. Benzing, T., Yaffe, M. B., Arnould, T., Sellin, L., Schermer, B., Schilling, B., Schreiber, R., Kunzelmann, K., Leparc, G. G., Kim, E., and Walz, G. (2000) *J. Biol. Chem.* **275,** 28167–28172
9. De Vries, L., Lou, X., Zhao, G., Zheng, B., and Farquhar, M. G. (1998) *Proc. Natl. Acad. Sci. U. S. A.* **95,** 12340–12345
10. Carman, C. V., Parent, J. L., Day, P. W., Pronin, A. N., Sternweis, P. M., Wedegaertner, P. B., Gilman, A. G., Benovic, J. L., and Kozasa, T. (1999) *J. Biol. Chem.* **274,** 34483–34492
11. Usui, H., Nishiyama, M., Moroi, K., Shibasaki, T., Zhou, J., Ishida, J., Fukamizu, A., Haga, T., Sekiya, S., and Kimura, S. (2000) *Int. J. Mol. Med.* **5,** 335–340
12. Sallese, M., Mariggio, S., D'Urbano, E., Iacovelli, L., and De Blasi, A. (2000) *Mol. Pharmacol.* **57,** 826–831
13. Schiff, M. L., Siderovski, D. P., Jordan, J. D., Brothers, G., Snow, B., De Vries, L., Ortiz, D. F., and Diverse-Pierluissi, M. (2000) *Nature* **408,** 723–727
14. Hart, M. J., Jiang, X., Kozasa, T., Roscoe, W., Singer, W. D., Gilman, A. G., Sternweis, P. C., and Bollag, G. (1998) *Science* **280,** 2112–2114
15. Kozasa, T., Jiang, X., Hart, M. J., Sternweis, P. M., Singer, W. D., Gilman, A. G., Bollag, G., and Sternweis, P. C. (1998) *Science* **280,** 2109–2111
16. Schultz, J., Copley, R. R., Doerks, T., Ponting, C. P., and Bork, P. (2000) *Nucleic Acids Res.* **28,** 231–234
17. Koelle, M. R., and Horvitz, H. R. (1996) *Cell* **84,** 115–125
18. Hoffman, G. A., Garrison, T. R., and Dohlman, H. G. (2000) *J. Biol. Chem.* **275,** 37533–37541
19. Lockhart, D. J., and Winzeler, E. A. (2000) *Nature* **405,** 827–836
20. Uetz, P., Giot, L., Cagney, G., Mansfield, T. A., Judson, R. S., Knight, J. R., Lockshon, D., Narayan, V., Srinivasan, M., Pochart, P., Qureshi-Emili, A., Li, Y., Godwin, B., Conover, D., Kalbfleisch, T., Vijayadamodar, G., Yang, M., Johnston, M., Fields, S., and Rothberg, J. M. (2000) *Nature* **403,** 623–627
21. Ito, T., Chiba, T., Ozawa, R., Yoshida, M., Hattori, M., and Sakaki, Y. (2001) *Proc. Natl. Acad. Sci. U. S. A.* **98,** 4569–4574
22. Pandey, A., and Mann, M. (2000) *Nature* **405,** 837–846
23. Gavin, A. C., Bosche, M., Krause, R., Grandi, P., Marzioch, M., Bauer, A., Schultz, J., Rick, J. M., Michon, A. M., Cruciat, C. M., Remor, M., Hofert, C., Schelder, M., Brajenovic, M., Ruffner, H., Merino, A., Klein, K., Hudak, M., Dickson, D., Rudi, T., Gnau, V., Bauch, A., Bastuck, S., Huhse, B., Leutwein, C., Heurtier, M. A., Copley, R. R., Edelmann, A., Querfurth, E., Rybin, V., Drewes, G., Raida, M., Bouwmeester, T., Bork, P., Seraphin, B., Kuster, B., Neubauer, G., and Superti-Furga, G. (2002) *Nature* **415,** 141–147
24. Gygi, S. P., Rist, B., Gerber, S. A., Turecek, F., Gelb, M. H., and Aebersold, R. (1999) *Nat. Biotechnol.* **17,** 994–999
25. Verma, R., Chen, S., Feldman, R., Schieltz, D., Yates, J., Dohmen, J., and Deshaies, R. J. (2000) *Mol. Biol. Cell* **11,** 3425–3439
26. Ho, Y., Gruhler, A., Heilbut, A., Bader, G. D., Moore, L., Adams, S. L., Millar, A., Taylor, P., Bennett, K., Boutilier, K., Yang, L., Wolting, C., Donaldson, I., Schandorff, S., Shewnarane, J., Vo, M., Taggart, J., Goudreault, M., Muskat, B., Alfarano, C., Dewar, D., Lin, Z., Michalickova, K., Willems, A. R., Sassi, H., Nielsen, P. A., Rasmussen, K. J., Andersen, J. R., Johansen, L. E., Hansen, L. H., Jespersen, H., Podtelejnikov, A., Nielsen, E., Crawford, J., Poulsen, V., Sorensen, B. D., Matthiesen, J., Hendrickson, R. C., Gleeson, F., Pawson, T., Moran, M. F., Durocher, D., Mann, M., Hogue, C. W., Figeys, D., and Tyers, M. (2002) *Nature* **415,** 180–183
27. Winzeler, E. A., Shoemaker, D. D., Astromoff, A., Liang, H., Anderson, K., Andre, B., Bangham, R., Benito, R., Boeke, J. D., Bussey, H., Chu, A. M., Connelly, C., Davis, K., Dietrich, F., Dow, S. W., El Bakkoury, M., Foury, F., Friend, S. H., Gentalen, E., Giaever, G., Hegemann, J. H., Jones, T., Laub, M., Liao, H., Davis, R. W., *et al.* (1999) *Science* **285,** 901–906
28. Boulton, S. J., Gartner, A., Reboul, J., Vaglio, P., Dyson, N., Hill, D. E., and Vidal, M. (2002) *Science* **295,** 127–131
29. Ausubel, F. M., Brent, R., Kingston, R. E., Moore, D. D., Seidman, J. G., Smith, J. A., and Struhl, K. (eds) (1987) *Current Protocols in Molecular Biology*, Greene/Wiley-Interscience, New York
30. Dohlman, H. G., Song, J., Ma, D., Courchesne, W. E., and Thorner, J. (1996) *Mol. Cell. Biol.* **16,** 5194–5209
31. Sikorski, R. S., and Hieter, P. (1989) *Genetics* **122,** 19–27
32. Song, J., Hirschman, J., Gunn, K., and Dohlman, H. G. (1996) *J. Biol. Chem.* **271,** 20273–20283
33. Dohlman, H. G., Apaniesk, D., Chen, Y., Song, J., and Nusskern, D. (1995) *Mol. Cell. Biol.* **15,** 3635–3643
34. Stevenson, B. J., Rhodes, N., Errede, B., and Sprague, G. F., Jr. (1992) *Genes Dev.* **6,** 1293–1304
35. Cagney, G., Uetz, P., and Fields, S. (2000) *Methods Enzymol.* **328,** 3–14
36. Wodicka, L., Dong, H., Mittmann, M., Ho, M. H., and Lockhart, D. J. (1997) *Nat. Biotechnol.* **15,** 1359–1367
37. Hill, A. A., Hunter, C. P., Tsung, B. T., Tucker-Kellogg, G., and Brown, E. L. (2000) *Science* **290,** 809–812

38. Moskvina, E., Schuller, C., Maurer, C. T., Mager, W. H., and Ruis, H. (1998) *Yeast* **14,** 1041–1050
39. Roth, F. P., Hughes, J. D., Estep, P. W., and Church, G. M. (1998) *Nat. Biotechnol.* **16,** 939–945
40. Altschul, S. F., Madden, T. L., Schaffer, A. A., Zhang, J., Zhang, Z., Miller, W., and Lipman, D. J. (1997) *Nucleic Acids Res.* **25,** 3389–3402
41. Jeanmougin, F., Thompson, J. D., Gouy, M., Higgins, D. G., and Gibson, T. J. (1998) *Trends Biochem. Sci* **23,** 403–405
42. Page, R. D. (1996) *Comput. Appl. Biosci.* **12,** 357–358
43. Nakai, K., and Kanehisa, M. (1992) *Genomics* **14,** 897–911
44. Apanovitch, D. M., Slep, K. C., Sigler, P. B., and Dohlman, H. G. (1998) *Biochemistry* **37,** 4815–4822
45. Moskvina, E., Imre, E. M., and Ruis, H. (1999) *Mol. Microbiol.* **32,** 1263–1272
46. Martinez-Pastor, M. T., Marchler, G., Schuller, C., Marchler-Bauer, A., Ruis, H., and Estruch, F. (1996) *EMBO J.* **15,** 2227–2235
47. Schmitt, A. P., and McEntee, K. (1996) *Proc. Natl. Acad. Sci. U. S. A.* **93,** 5777–5782
48. Rep, M., Krantz, M., Thevelein, J. M., and Hohmann, S. (2000) *J. Biol. Chem.* **275,** 8290–8300
49. Marchler, G., Schuller, C., Adam, G., and Ruis, H. (1993) *EMBO J.* **12,** 1997–2003
50. Varela, J. C., Praekelt, U. M., Meacock, P. A., Planta, R. J., and Mager, W. H. (1995) *Mol. Cell. Biol.* **15,** 6232–6245
51. DiBello, P. R., Garrison, T. R., Apanovitch, D. M., Hoffman, G., Shuey, D. J., Mason, K., Cockett, M. I., and Dohlman, H. G. (1998) *J. Biol. Chem.* **273,** 5780–5784
52. Brewster, J. L., de Valoir, T., Dwyer, N. D., Winter, E., and Gustin, M. C. (1993) *Science* **259,** 1760–1763
53. Xu, B. E., Skowronek, K. R., and Kurjan, J. (2001) *Genetics* **159,** 1559–1571
54. Chen, T., and Kurjan, J. (1997) *Mol. Cell. Biol.* **17,** 3429–3439
55. Abeliovich, H., Grote, E., Novick, P., and Ferro-Novick, S. (1998) *J. Biol. Chem.* **273,** 11719–11727
56. Holthuis, J. C., Nichols, B. J., Dhruvakumar, S., and Pelham, H. R. (1998) *EMBO J.* **17,** 113–126
57. Becherer, K. A., Rieder, S. E., Emr, S. D., and Jones, E. W. (1996) *Mol. Biol. Cell* **7,** 579–594
58. Gerrard, S. R., Levi, B. P., and Stevens, T. H. (2000) *Traffic* **1,** 259–269
59. Nothwehr, S. F., Bryant, N. J., and Stevens, T. H. (1996) *Mol. Cell. Biol.* **16,** 2700–2707
60. Rothman, J. H., Howald, I., and Stevens, T. H. (1989) *EMBO J.* **8,** 2057–2065
61. Luo, W., and Chang, A. (2000) *Mol. Biol. Cell* **11,** 579–592
62. Luo, W., and Chang, A. (1997) *J. Cell Biol.* **138,** 731–746
63. Latterich, M., and Watson, M. D. (1991) *Mol. Microbiol.* **5,** 2417–2426
64. Latterich, M., and Watson, M. D. (1993) *Biochem. Biophys. Res. Commun.* **191,** 1111–1117
65. Garrison, T. R., Zhang, Y., Pausch, M., Apanovitch, D., Aebersold, R., and Dohlman, H. G. (1999) *J. Biol. Chem.* **274,** 36387–36391
66. Zheng, B., Ma, Y. C., Ostrom, R. S., Lavoie, C., Gill, G. N., Insel, P. A., Huang, X. Y., and Farquhar, M. G. (2001) *Science* **294,** 1939–1942
67. Dulic, V., and Riezman, H. (1990) *J. Cell Sci.* **97,** 517–525
68. Nomoto, S., Nakayama, N., Arai, K., and Matsumoto, K. (1990) *EMBO J.* **9,** 691–696
69. Cole, G. M., Stone, D. E., and Reed, S. I. (1990) *Mol. Cell. Biol.* **10,** 510–517
70. Whiteway, M., Hougan, L., and Thomas, D. Y. (1990) *Mol. Cell. Biol.* **10,** 217–222
71. Dolan, J. W., and Fields, S. (1990) *Genes Dev.* **4,** 492–502
72. Maeda, T., Takekawa, M., and Saito, H. (1995) *Science* **269,** 554–558
73. Raitt, D. C., Posas, F., and Saito, H. (2000) *EMBO J.* **19,** 4623–4631
74. Reiser, V., Salah, S. M., and Ammerer, G. (2000) *Nat. Cell Biol.* **2,** 620–627
75. Inoue, Y., Tsujimoto, Y., and Kimura, A. (1998) *J. Biol. Chem.* **273,** 2977–2983
76. Estruch, F., and Carlson, M. (1993) *Mol. Cell. Biol.* **13,** 3872–3881
77. Gorner, W., Durchschlag, E., Martinez-Pastor, M. T., Estruch, F., Ammerer, G., Hamilton, B., Ruis, H., and Schuller, C. (1998) *Genes Dev.* **12,** 586–597
78. Thevelein, J. M., and de Winde, J. H. (1999) *Mol. Microbiol.* **33,** 904–918
79. Tadi, D., Hasan, R. N., Bussereau, F., Boy-Marcotte, E., and Jacquet, M. (1999) *Yeast* **15,** 1733–1745
80. Reineke, U., Volkmer-Engert, R., and Schneider-Mergener, J. (2001) *Curr. Opin. Biotechnol.* **12,** 59–64
81. Petiot, A., Ogier-Denis, E., Bauvy, C., Cluzeaud, F., Vandewalle, A., and Codogno, P. (1999) *Biochem. J.* **337,** 289–295
82. De Vries, L., Elenko, E., McCaffery, J. M., Fischer, T., Hubler, L., McQuistan, T., Watson, N., and Farquhar, M. G. (1998) *Mol. Biol. Cell* **9,** 1123–1134
83. Wylie, F., Heimann, K., Le, T. L., Brown, D., Rabnott, G., and Stow, J. L. (1999) *Am. J. Physiol.* **276,** C497–C506
84. Ogier-Denis, E., Pattingre, S., El Benna, J., and Codogno, P. (2000) *J. Biol. Chem.* **275,** 39090–39095
85. Sato, T. K., Overduin, M., and Emr, S. D. (2001) *Science* **294,** 1881–1885
86. Kamura, T., Burian, D., Khalili, H., Schmidt, S. L., Sato, S., Liu, W. J., Conrad, M. N., Conaway, R. C., Conaway, J. W., and Shilatifard, A. (2001) *J. Biol. Chem.* **276,** 16528–16533
87. Schmidt, A. E., Miller, T., Schmidt, S. L., Shiekhattar, R., and Shilatifard, A. (1999) *J. Biol. Chem.* **274,** 21981–21985
88. Shilatifard, A., Lane, W. S., Jackson, K. W., Conaway, R. C., and Conaway, J. W. (1996) *Science* **271,** 1873–1876
89. Yeghiayan, P., Tu, J., Vallier, L. G., and Carlson, M. (1995) *Yeast* **11,** 219–224
90. Joazeiro, C. A., and Weissman, A. M. (2000) *Cell* **102,** 549–552
91. Melchior, F., and Gerace, L. (1998) *Trends Cell Biol.* **8,** 175–179
92. Nigg, E. A. (1997) *Nature* **386,** 779–787
93. Schultz, J., Milpetz, F., Bork, P., and Ponting, C. P. (1998) *Proc. Natl. Acad. Sci. U. S. A.* **95,** 5857–5864